ELSEVIER

Wear 209 (1997) 284–291

WEAR

Modeling of jetflow drilling with consideration of the chaotic erosion histories of particles

Z. Yong, R. Kovacevic

Center for Robotics and Manufacturing Systems, University of Kentucky, Lexington, KY 40506-0108, USA

Received 24 October 1996; accepted 5 February 1997

Abstract

A general model is presented for the simulation of a drilling process by abrasive waterjet. The conventional constitutive equation for the erosion rate of a single particle penetrating into a solid target is extended and applied to millions of particle strikes, taking into consideration their erosion histories. The theoretical advancement of this model reflects the inherent damping effect that occurs as the depth of drilling increases. Particles involved in erosion are divided into categories according to their kinematic features, and their penetration performances are evaluated individually. A particle-laden jetflow with chaotic behavior, which was constructed previously by the authors, is employed to coordinate the positions of particles and describe their velocities and flow rates, including laminar and turbulent flow with the average scale. The high accuracy of the theoretical results is verified by independent experiments of drilling glass, titanium and other materials. © 1997 Elsevier Science S.A.

Keywords: Jetflow drilling; Chaotic erosion

1. Introduction

It is difficult to drill deep and small holes in hard-to-machine materials like titanium and brittle ceramics. A recent development in abrasive waterjet (AWJ) technology provides a new alternative machining tool to carry out such an operation on the shop floor [1]. Similar to other AWJ machining processes, in AWJ drilling, millions of high-speed particles (40–400 m s^{-1}) strike the target every few seconds and remove material little by little. For a ductile material, a particle can cut much like a traditional machining tool [2–4], while for a brittle material it penetrates into the target through fragmentation [5,6]. Craters and ditches produced by the impact of particles are visible with a microscope as displayed in Figs. 1 and 2. Possibly owing to the complexity of impact processes, to date the authors are unaware of any

Fig. 1. Craters (×130) on the surface of a glass specimen generated by two particles through fragmentation.

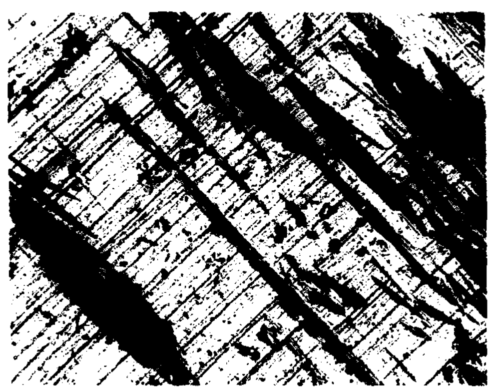

Fig. 2. Ditches (×98) on the surface of a titanium specimen produced by particles through cutting.

0043-1648/97/$17.00
PII S0043-1648(97)00032-X

model for the three-dimensional drilling process which can evaluate the erosive contribution of every individual particle.

The modeling of AWJ drilling can serve at least two practical purposes. First, the off-line simulation prior to the online operation can help engineers choose optimal parameters that will yield low cost and high quality. Second, if on-line control is required, an accurate robust model is necessary in association with the sensor and controllers to form a closed-loop control system.

In general, three steps are needed for the development of an accurate model: (1) kinematic analysis of abrasive particles in multiphase jetflow, (2) establishment of the constitutive law for the particle–target interaction, and (3) evaluation of drilling performance conducted by millions of particles. Extensive investigations have been implemented by the authors for simulation of particle motion on the cross-section of particle-laden flow [7–9], therefore the attention here is turned to the derivation of constitutive equations and the computation of the geometrical configuration of a hole. The theoretical analysis is verified by independent experiments of drilling glass, titanium and other materials.

2. Constitutive equation

The relation between the average depth of penetration caused by the impact of a single particle and other machining parameters is defined as the constitutive equation of particle–target interaction during erosion. Great efforts have been made in the past decades to build this type of relation to evaluate accurately the erosion rate for machining purposes.

Extensive theoretical and experimental investigations show that the average depth of penetration h_a on the dry surface of a ductile material can be expressed by

$$h_a = \lambda_1 V^{\lambda_2} \tag{1}$$

where V is the velocity of the particle, $\lambda_1 > 0$ and $\lambda_2 > 0$ are constants relevant to material properties, impact angle, and contact geometry of the particle and target [2–6,10–14].

Eq. (1) is based on metal cutting dynamics and the Hertz impact contact theory [2,10–12] which lead to the relation between the average removal volume Q_a and the velocity V of a particle

$$Q_a = E_1 V^{E_2} \tag{2}$$

where E_1 and E_2 are constants. The conversion of Eq. (2) to Eq. (1) is basically a geometric process rather than a physical process. Today the constitutive Eq. (1) is widely accepted by the researchers in this area as a classical relation. However, it is very important to point out that Eq. (1) is confined by several limitations. For example, Eq. (1) no longer holds when a film exists between two contact bodies. In addition, it is independent from erosion histories of other particles. As a matter of fact, the latest studies [14,15] show that the impact force will be reduced if a moving object encounters a soft film before penetrating into a target. For the one-phase liquid film, the relation between the impact force P_I and the thickness H of the film is given by

$$P_I \rightarrow \frac{1}{H^2} \tag{3}$$

derived from a fluid mechanics approach [15]. When the film consists of the mixture of solid and liquid, the relation is of the form

$$P_I \rightarrow \frac{1}{H^{\alpha}} \tag{4}$$

where α is a physical constant. Eq. (4) is deduced from the Hertz impact contact theory for two inhomogeneous bodies [14].

The thickness of the film between a particle and the target is likely to increase with the increase of depth of drilling. Therefore, the impact force varies simultaneously with the change. This suggests that the classical relation Eq. (1) needs modifying before being applied to calculate the erosion rate of a particle in AWJ drilling. In doing so, two basic assumptions are introduced as follows.

- The form of Eq. (1) is invariable under any erosion conditions provided that λ_1 and λ_2 are functions of the drilling depth.
- Eq. (1) is also suitable for brittle materials if the material fragmentation caused by impact takes place only within the immediate area.

In deriving the relation between the depth of penetration and relevant parameters, one critical concern is that its mathematical statement must be concise in addition to accuracy, so as to reduce computation time. As shown in Fig. 3, the surface of a target material to be drilled is divided into a finite element network. During the erosion, each element acts as a memory-cell to record the histories of those particles which pass through it and hit the target surface. As shown in Fig. 3, when the jth particle trapped by the ith cell at instant t_j strikes the surface, based on the above assumptions, the constitutive equation for the average penetration depth is generalized to

$$\delta h_j = \lambda_1(h_{j-1})\,[V_j(r_i,\theta_i)]^{\lambda_2(h_{j-1})} \tag{5}$$

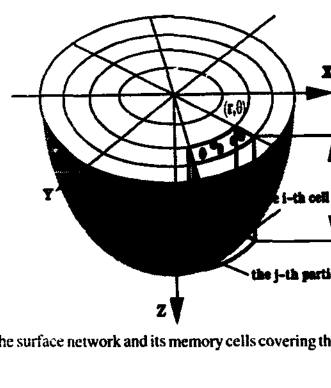

Fig. 3. The surface network and its memory cells covering the drilling region.

Here h_{j-1} ($j>1$) is the depth of penetration by $j-1$ particles prior to the jth particle in the ith cell centered by (r_i,θ_i), $V_j=v_j/v_{max}$ ($0\le V_j\le 1$) is the dimensionless ongoing velocity of the jth particle right after it exits from the nozzle, v_j is its real velocity and v_{max} is the maximum velocity of particles in the jetflow. Without loss of generality, the radius produced by ongoing flow is taken as the unit radius while the cross-sectional thickness of the ring-shaped outgoing flow is denoted by δ_t. The final theoretical radius of a hole is $1+\delta_t$.

It is very important to point out that, like the constitutive equations in continuum mechanics [16], $\lambda_1(h_{j-1})$ and $\lambda_2(H_{j-1})$ in Eq. (5) are not arbitrary functions of h_{j-1} but are constrained strictly by various physical principles. To find appropriate explicit forms of $\lambda_1(h_{j-1})$ and $\lambda_2(h_{j-1})$, a comprehensive analysis on these constraints is necessary.

Differentiating δh_j of Eq. (5) with respect to h_{j-1} leads to

$$\frac{d(\delta h_j)}{dh_{j-1}}=V_j^{\lambda_2}\left(\frac{d\lambda_1}{dh_{j-1}}+\lambda_1 \ln V_j\frac{d\lambda_2}{dh_{j-1}}\right) \tag{6}$$

Since δh_j decreases when h_{j-1} increases and the damping effects are not negligible, $d(\delta h_j)/dh_{j-1}\le 0$ holds during erosion. Then Eq. (6) produces

$$\frac{d\lambda_1}{dh_{j-1}}+\lambda_1\frac{d\lambda_2}{dh_{j-1}}\ln V_j\le 0 \quad (V_j\ne 0) \tag{7}$$

and furthermore

$$\frac{d\lambda_1}{dh_{j-1}}\le \lambda_1\frac{d\lambda_2}{dh_{j-1}}|\ln V_j| \tag{8}$$

owing to $\ln V_j\le 0$. Eq. (8) is a constraint on the relation among λ_1, λ_2 and V_j; further examination is necessary to find a more specific constraint on λ_1.

At the center of the jet, the dimensionless velocity V_j reaches its maximum value $V_j=1$, and hence $|\ln V_j|$ reads its minimum $|\ln V_j|=0$. Additionally, $\lambda_1 d\lambda_1/dh_{j-1}$ and $d\lambda_2/dh_{j-1}$ are both independent of V_j, therefore, the inequality

$$\frac{d\lambda_1}{dh_{j-1}}\le 0 \tag{9}$$

must hold as a general constraint on the function $\lambda_1(h_{j-1})$ of constitutive Eq. (5). Another constraint on $\lambda_1(h_{j-1})$ is that it is bounded at any circumstance including $h_{j-1}=0$.

For ductile materials, the constraint $\lambda_2(h_{j-1})\approx 2$–$2.3$ appears to be true, in most cases, according to many investigations [2,3,6,10–13]. A constraint on the function $\lambda_2(h_{j-1})$ for brittle materials can be derived from the energy conservation principle. Without loss of generality, the area of the new surface generated by the impact of the jth particle is written as $S_f(\delta h_{j-1})^2$ where S_f is the geometric transforming coefficient. For example, one can find $S_f=2\pi$ if the crater is assumed to have a semispherical shape. The surface energy consumed by the formation of the new surface is $E_s=\gamma_0 S_f(\delta h_{j-1})^2$, where γ_0 is the surface energy density.

Multiplying Eq. (5) by $\gamma_0 S_f \delta h_{j-1}$ yields

$$E_s=\gamma_0 S_f(\delta h_{j-1})^2=S_f\gamma_0\lambda_1^2 V_j^{2\lambda_2}<\tfrac{1}{2}m_p V_j^2 \tag{10}$$

where m_p is the mass of the particle. The physical meaning of Eq. (10) is that the surface energy consumed by brittle fragmentation is less than the total kinetic energy of the particle. Based on the energy conservation principle, from another form of Eq. (10)

$$\lambda_1^2 V_j^{2(\lambda_2-1)}<\frac{m_p}{2S_f\gamma_0} \tag{11}$$

one can confirm that the constraint

$$\lambda_2(h_{j-1})\ge 1 \tag{12}$$

must hold. Otherwise when $V_j\to 0$ the condition

$$V_j^{2(\lambda_2-1)}\to\infty \tag{13}$$

leads to a conclusion against a fundamental law if $\lambda_2(h_{j-1})<1$.

Based on Eqs. (3) and (4) and inequality Eq. (9), the forms of λ_1 and λ_2 are chosen as

$$\lambda_1=\frac{l_3}{h_{j-1}^{l_1}+l_2},\ \lambda_2=l_4 h_{j-1}+2 \quad (l_1\ge 1,\ l_2,\ l_3>0,\ l_4>-1) \tag{14}$$

where l_i ($i=1$–4) are constants. The constant l_2 is introduced for ensuring that λ_1 is bounded when $h_{j-1}=0$. Here $l_1\ge 1$ is required because the first-order differentiation of λ_1

$$\frac{d\lambda_1}{dh_{j-1}}=-\frac{l_3 l_1 h_{j-1}^{l_1-1}}{(h_{j-1}^{l_1}+l_2)^2} \tag{15}$$

must be bounded when $h_{j-1}\to 0$.

The final form of the constitutive equation is

$$\delta h_j=\frac{l_3}{h_{j-1}^{l_1}+l_2}[V_j(r_i,\theta_i)]^{l_4 h_{j-1}+2} \tag{16}$$

It will be seen that the unknown constants l_i ($i=1$–4) will be reduced from four to one. In Eq. (14), the physical meaning of l_3/l_2 can be clarified by setting $j=1$ at the center of a hole, namely, $h_1=\delta h_1=l_3/l_2$ owing to $h_0=0$ and $V_j=1$. l_1 is a parameter to reflect damping effects, and l_4 is a parameter that controls the shape of a hole and it is independent of the maximum depth of penetration.

Intuitively, the deeper a hole is, the thicker the film between two contact bodies should be. Therefore, in comparison with Eqs. (3) and (4), the following expressions are chosen for l_i ($i=1$–4)

$$l_1=2,\ l_3=l_2 l=l^3,\ l_4=0.2/l \tag{17}$$

where $l>0$ is a constant. As a result, Eq. (16) is rewritten in the dimensionless form

$$\delta\bar{h}_j=\frac{1}{\bar{h}_{j-1}^2+1}[V_j(r_i,\theta_i)]^{0.2\bar{h}_{j-1}+2} \tag{18}$$

with

$$\bar{h}_{j-1}=h_{j-1}/l \quad \delta\bar{h}_j=\delta h_j/l \tag{19}$$

According to the result in [2], the expression of average constant incoming velocity V_j^* with damping effects works out to be $V_j^* = V_j/(a+bh_{j-1})$ where a and b are constants. The information contained in Eq. (18) reflects a similarity from this parameter if $V_j/(\bar{h}_{j-1}^2+1)^{1/(0.2\bar{h}_{j-1}+2)}$ is defined as the incoming velocity.

One remarkable feature of Eq. (18) is that it only has one unknown parameter l, which can be determined by combining theoretical modeling with the test of drilling a hole in the material to be machined.

3. Category of particles

Before evaluating the depth of penetration corresponding to a memory cell defined in Fig. 3, it is imperative to know the number of particles which pass through a memory cell and effectively contact the target material. In doing so, the criterion for trapping particles in the ith cell is introduced in the forms

$$|r_i - r_j| \le \frac{\Delta r}{2} \quad |\theta_i - \theta_j| \le \frac{\Delta\theta}{2} \tag{20}$$

where (r_j, θ_j) are the coordinates of a particle at a given instant, Δr is the radial increment of the cell network and $\Delta\theta$ is the angular increment. Note that Eq. (20) can be a necessary and sufficient condition for effective erosion only if a particle hits the target. Otherwise it is only a necessary condition because some particles rebounding from the previous impact may pass over the area covered by the i-th cell but not strike it.

All the particles recorded by a cell are defined as a point set Ω. In terms of the roles of particles in erosion, Ω is divided into two subsets, Ω_1 and Ω_2. The particles striking the surface directly are categorized into Ω_1, and the particles rebounding from the previous impact belong to group Ω_2. Obviously,

$$\Omega_1 \cap \Omega_2 = \varnothing \quad \Omega_1 \cup \Omega_2 = \Omega \tag{21}$$

hold under the classification. For the sake of accurate calculations, further divisions of Ω_1 and Ω_2 are necessary.

As shown in Fig. 4, Ω_1 is divided into many subsets and they yield the relations

$$\omega_1 \cap \omega_2 \cap \ldots \cap \omega_K = \varnothing \quad \omega_1 \cup \omega_2 \cup \ldots \cup \omega_K = \Omega_1 \tag{22}$$

One criterion for the division of Eq. (22) is that particles in a subset are sufficient to cover the area of the cell and to remove a layer of the target material. In addition, particles in the subset ω_{k-1} $(1<k<K)$ enter into the cell earlier than particles in ω_k. The classification is essential in applying constitutive Eq. (16) or Eq. (18) to the evaluation of penetration rates of particles.

Usually a particle of Ω_2 carries much less energy than a particle in Ω_1 does, or in other words, the particles of Ω_1 remove material much more efficiently than particles of Ω_2. In comparison with their performance in deep cutting, the particles of Ω_2 play a less important role in drilling a hole. The rationale for this reasoning is that there is no way for a particle of Ω_2 to escape other than the ring-like channel of backflow neighboring on the lateral surface of a hole. As a result, a particle of Ω_2 can hardly generate an effective secondary impact because of the resistance of incoming flow.

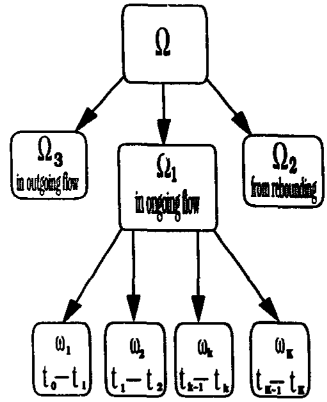

Fig. 4. Classification of particles.

In particular, when a cell is located on the boundary, its particles, denoted by Ω_3, are transported by backflow. The criterion Eq. (20) becomes

$$|r_i - (1+\delta_i)| \le \frac{\Delta r}{2}, \quad |\theta_i - \theta_j| \le \frac{\Delta\theta}{2} \tag{23}$$

In this case, Ω_1 does not exist. However, only these particles contacting the lateral surface of a hole can erode the target, and the majority of them in backflow exits from the annular channel without contacting the target.

4. Source of particles

If there is no theoretical particle source of the jetflow with specific coordinates and velocity profiles, it is impossible to model a drilling process by use of the above theoretical results. Theoretically speaking, a useful particle source is a point set that possesses the following essential conditions.

- The order of appearance of particles on the cross-section of the jetflow is randomly disordered or chaotic with respect to either the location or time.
- After the number of particles passing through the cross-section exceeds a certain value, the particle distribution should approach the axisymmetrical status. In other words, the three-phase jetflow appears to be geometrically axisymmetrical.
- The particles should be endowed with any desired velocity profile and flow rate so that they are adaptable to variable machining conditions.

A novel approach has been developed by the authors to construct such particle sources [7–9]. The patterns of a par-

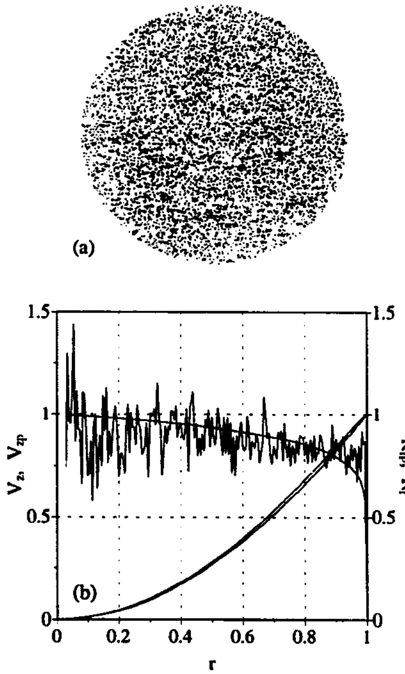

Fig. 5. (a) Particle distribution on the cross-section of the jetflow ($n=7202$). (b) The velocity profile and flow rate ratio of particles compared with the known results.

ticle distribution and its velocity profile are shown in Fig. 5. The variable V_{zp} for a desired point set with the oscillation characteristic is the dimensionless velocity profile calculated by particle distribution, and $V_z=(1-r)^{1/7}$ with smooth curvature is its theoretical value given as the known condition. R_{fp} and R_f are flow rate ratios with respect to V_{zp} and V_z respectively.

Based on the simulation results [7–9], positions of particles are known despite their disordered property over the erosion region and hence a cell can trap the particles passing through it based on the criterion Eq. (20). When the number of particles that the cell receives reaches the designated value, constitutive Eq. (18) can be used to evaluate, step by step, the erosion rate.

Two typical physical parameters of a particle source are its velocity profile and flow rate ratio. In modeling a drilling process, two types of velocity profile and flow rate ratio are used to describe the kinematic manners of particles [17–19]. One comes from laminar flow with

$$V_j=1-r_i^2,\ R_f=r_i^2(2-r_i^2) \tag{24}$$

where R_f stands physically for the flow rate ratio; the other results from the seventh root law for turbulent flow

$$V_j=(1-r_i)^{1/7},\ R_f=1-(1-r_i)^{8/7}\left(1+\tfrac{8}{7}r_i\right) \tag{25}$$

The physical meaning of R_f is the intensity of the number of particles passing through a specific region during a time interval.

5. Modeling and experiment

The central task of modeling is to determine the erosion rates of particles in every cell. In the present work, the particles of Ω_2 are not evaluated theoretically because it is very difficult to estimate their exact number and velocity distribution, but their effects are counted by experimental constants l_i ($i=1$–4). In addition, particles in Ω_3 in backflow are assumed to enlarge only proportionally the diameter of a hole generated by particles of Ω_1, and hence they are independent of the shape and depth of a hole. Consequently, only the particles of Ω_1 are taken into account owing to their high energy status.

Substitution of the first equation in Eq. (24) and Eq. (25) into Eq. (18) respectively leads to two equations

$$\delta\bar{h}_j=\frac{1}{\bar{h}_{j-1}^2+1}(1-r_i^2)^{0.2\bar{h}_{j-1}+2} \tag{26}$$

for laminar jetflow and

$$\delta\bar{h}_j=\frac{1}{\bar{h}_{j-1}^2+1}(1-r_i)^{(1/7)(0.2\bar{h}_{j-1}+2)} \tag{27}$$

for turbulent jetflow, where $\bar{h}_{j-1}=\bar{h}_{j-1}(\omega_i)$ ($i=2,\ldots,K$) is the function of the point set ω_i with respect to a specific cell.

An example is given here to illustrate how to model the drilling process by means of the above theoretical results. Suppose that a cell receives 100 strikes during an entire erosion process. The particles are equally divided into four portions, that is, $\omega_1=\omega_2=\omega_3=\omega_4=25$. After substitution of radii r_i of the first 25 particles into Eq. (26) or Eq. (27) of $h_0=0$ ($j=1$) to calculate the depth of penetration produced by every particle, one obtains the average depth of drilling by dividing the sum of the penetrations of the 25 particles by 25. The result is taken as the depth $\bar{h}_1$ of Eq. (26) or Eq. (27). During computation of the average depth generated by the second 25 particles, $\bar{h}_1$ is used to compute the average removal of the second layer. Repeating this procedure, one gains the final depth $\bar{h}_f$ of penetration by 100 particles in the cell by adding them together as

$$\bar{h}_f=\sum_{k=1}^{4}\delta\bar{h}_k=\sum_{k=1}^{4}\frac{1}{\bar{h}_{k-1}^2+1}[V_k(r_i)]^{0.2\bar{h}_{j-1}+2}\quad (h_0=0) \tag{28}$$

Note that the constant l is contained in Eq. (28). After the penetration of all the cells is found, the shape of the hole is the accumulation of all the depths covering the drilling area.

From Eqs. (18) and (19), one may think that the equation $\delta h_1=l$ for the central depth of a hole ($r_i=0$) can be used to determine the value of l in association with an experimental result. However, it is found that theoretical results can be improved if it is ascertained by a maximum depth of drilling. In addition, it is difficult to estimate the initial depth h_1 of drilling.

An extended application of the model is to serve the closed loop control of a drilling operation [10,20], which requires that the model has the capability to respond rapidly. Additionally, the minimal computation can also lead to high efficiency and convenience for the shop floor. For practical purposes the analogous method described below is developed.

The cell analyzed here is located at the center of a hole with the maximum depth of penetration. Corresponding to $\{\omega_1,\omega_2,\ldots,\omega_j\}=\Omega_1$, a group of depths is determined and listed as $\{\bar{h}_1,\bar{h}_2,\ldots,\bar{h}_j\}$ for the cell. After the experiment gives the maximum or final depth h_{max} and the time t_{max}, the constant l can be determined by

$$\bar{h}_j l = h_j = h_{max} \rightarrow l = h_{max}/\bar{h}_j \tag{29}$$

and therefore

$$(h_1,h_2,\ldots,h_{j-1}) = l(\bar{h}_1,\bar{h}_2,\ldots,\bar{h}_{j-1}) \tag{30}$$

A nominated abrasive flow rate $\dot{m}$ is introduced to calculate the instant of penetrating a depth, given by

$$\dot{m} = n(\Omega_1)/t_{max} \tag{31}$$

where $n(\Omega_1)$ is the total number of particles in Ω_u. Consequently, a group of instants is determined by

$$(t_1,t_2,\ldots,t_{j-1}) = [n_1(\omega_1),n_2(\omega_1+\omega_2),\ldots, n_{j-1}(\omega_1+\omega_2+\ldots+\omega_{j-1})]/\dot{m} \tag{32}$$

where n_k $(1\leq k\leq j-1)$ is the sum of particles in the k subsets. As a result, one can verify and further predict the depth of drilling in terms of the one-to-one correspondence $\{(h_1,t_1),(h_2,t_2),\ldots,(h_{j-1},t_{j-1})\}$.

The most important feature of this approach is that the general relation between the depth of penetration and the time can be found without specific constraints on machining parameters, such as the abrasive flow rate and material properties. All other potential influences are included in the constant l.

The effectiveness of this model has been justified by many 'blind tests'. That is, after carrying out independent drilling experiments, someone else tells the authors a pair of data $(h_{max},t_{max})=(h_j,t_j)$. With the aid of the model, the authors can quickly give the rest of the results: $(h_1,t_1),(h_2,t_2),\ldots,(h_{j-1},t_{j-1})$. It should be noted that no other parameters are required, such as water pressure, materials of target and abrasive, abrasive flow rate and so on.

Two patterns are given in Fig. 6 to show the geometrical configurations of holes resulting from the simulation. To simplify numerical treatments, the axisymmetrical property of flow is employed to reduce the number of memory cells. For the simulation of drilling glass and titanium, 20 cells are designed over the erosion region and the particles within each cell are divided into 10 groups. The number of cells and the group number of particles in each cell are chosen such that the craters produced by particles can cover the area of a cell and a moderate increase or decrease in the two numbers does not have any significant influence on the theoretical erosion rate. If one wishes to scrutinize the surface characteristics caused by the chaotic behavior, size and shape of particles, more cells are needed and their sizes must be smaller. The axisymmetrical property of jetflow cannot be utilized at the local zone in this circumstance.

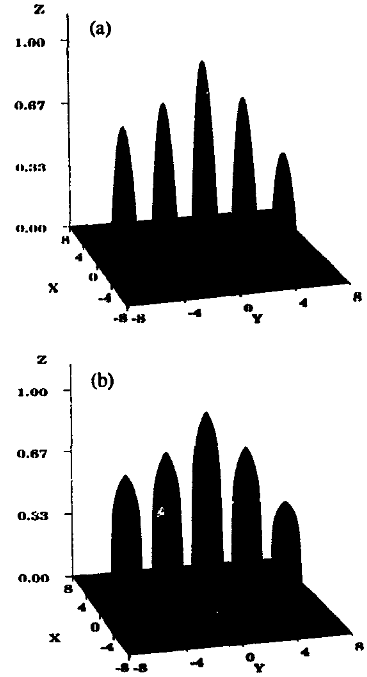

Fig. 6. (a) Shapes of five holes produced by theoretical laminar jetflow. (b) Shapes of five holes produced by theoretical turbulent flow (average scale).

The experimental verification of the geometry of a hole is given for glass in Fig. 7 Because of the existence of a groove on the surface of the glass specimen with the dimensions $200\times200\times75$ mm, the shape of the hole is distorted in the middle part in Fig. 7(a). This distortion is not seen in Fig. 7(b) after changing the viewing angle. The five holes are drilled by low speed flow which is possibly laminar flow since the waterjet pressure assigned in the experiments is as low as 50 MPa. Thus its theoretical counterpart is the pattern displayed in Fig. 6(a). For titanium, the shape of a hole is not directly visible but it appears to have similarity with the holes shown in Fig. 6(b). It can be seen that the shape of a hole depends mainly on the velocity profile of jetflow. As assumed before, backflow may proportionally enlarge the

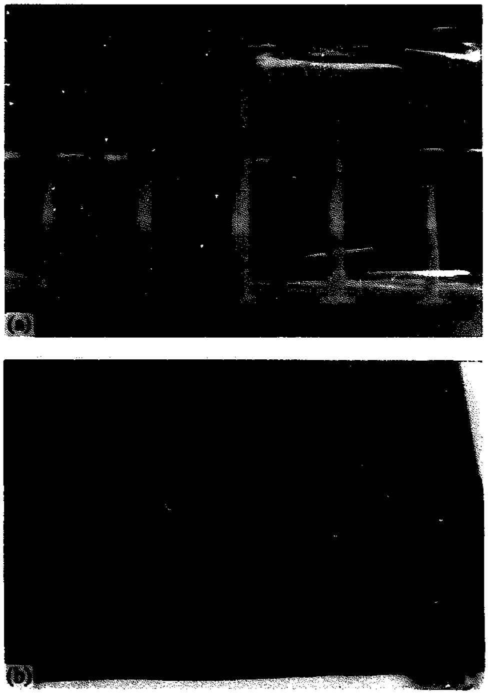

Fig. 7. (a) Five holes from experiments with 50 MPa water pressure. (b) Another view of the five holes in (a) from a different angle.

Table 1
Comparison between theory and experiment for drilling glass

	t (s)			
	30	40	60	90
h_e (mm)	32–33	39–40	45–46	55–56
h_t (mm)	35.5	40.1	47.1	55.0

Workpiece material, glass; abrasive material, aluminum oxide; size of abrasives, 100 (mesh); diameter of mixing tube, 2.5 mm; waterjet pressure, 50 MPa; abrasive flow rate, 5.4 g s^{-1}; standoff distance, 25 mm; l_0 = 18.86, l_1 = 2.0, l_2 = 0.2.

diameter of a hole rather than significantly change its shape. Tables 1 and 2 exhibit the excellent consistency between the theoretical and experimental data of the maximum depth of drilling for two types of materials, where h_e and h_t represent experimental and theoretical results respectively.

6. Conclusion and discussion

Armed with the knowledge that the erosion of a material is produced by millions of particles with high speed, the model first focuses on the construction of a reasonable constitutive equation between the depth of erosion and other machining parameters. In attempting to find such a fundamental relation, the mathematical structure of a classical formula is assumed to be invariable but its parameters are generalized to be functions of the drilling depth. Subjected to the basic physical constraints, an explicit form of the constitutive equation is presented whose structure is confined within the rational range.

Table 2
Comparison between theory and experiment for drilling titanium

	t (s)					
	12	21	30	40	50	60
h_e (mm)	12–13	16–17	19–20	23–24	25–27	28–30
h_t (mm)	14.4	18.5	21.4	23.5	26.1	28.0

Workpiece material, titanium; abrasive material, aluminum oxide; size of abrasives, 100 (mesh); diameter of mixing tube, 2.5 mm; waterjet pressure, 240 MPa; abrasive flow rate, 5.4 g s^{-1}; standoff distance, 24 mm; l_0 = 9.63, l_1 = 2.0, l_2 = 0.2.

Emphasis is given not only to an individual particle, but also to many particles in a given small region. The importance of this attention lies in the fact that the macro visible shape of a hole is the erosive result of millions of particles with different kinetic behaviors. In other words, when a constitutive equation is established for a single particle, the estimation of macro erosion is not completed unless contributions of all particles are counted. Generally speaking, particles are divided into three types. One is transported directly by ongoing jetflow, one is transported by outgoing flow and the third is those particles rebounding from their previous strikes. The three types of particles are treated differently in the model.

All the efforts could be in vain if a particle source is not available which represents the particle laden flow exiting from the nozzle. A desired source of particles is constructed in the previous research work and it can be endowed with any velocity profile, flow rate and shape. When coordinates and velocities of particles are known, memory cells of the surface network over the erosion region can trap particles passing through them and their penetration abilities can be evaluated. The final result is the accumulation of contributions made by particles in all cells.

To have an efficient approach to the simulation, the analogous method is introduced to reduce computation time and storage space. From the comparison between theory and experiment, it is confirmed that the model has very good accuracy and is applicable to the shop floor. Nevertheless, if surface characterization is required, the influence of particle size and chaotic distribution should be considered in the model; naturally this will make the mathematical computations more complex.

Acknowledgements

This project is supported by the National Science Foundation under Grant DMI-9523010. Support is also given partially by the Allison Engine Company, the Turbine Airfoils Products Center of Pratt and Whitney, and the Flow International Corporation.

References

[1] M. Hashish, Drilling of small-diameter holes in sensitive materials, Jet Cutting Technol. 13 (1994) 409–424.
[2] I. Finnie, Erosion of surfaces by solid particles, Wear 3 (1960) 87–103.
[3] G.P. Tilly, W. Sage. The interaction of particles and material behavior in erosion process, Wear 16 (1970) 447–465.
[4] I.M. Hutchings, Deformation of metal surfaces by oblique impact of square plates, Int. J. Mech. Sci. 19 (1977) 45–52.
[5] A.G. Evans, M.E. Gulden, M. Rosenblatt, Impact damage in brittle materials in the elastic–plastic response regime, Proc. R. Soc. London Ser. A 361 (1978) 343–365.
[6] M.E. Gulden, Solid particle erosion of high technology ceramics, in: W.F. Alfer (ed.), ASTM STP664, ASTM, Philadelphia, PA, 1979, pp. 101–122.
[7] Z. Yong, R. Kovacevic, Fundamentals of constructing particle-laden jetflow by fractal point sets and predicting 3D solid-erosion rates, J. of Chaos, soliton and fractals, 8 (2) (1997) 207–220.
[8] Z. Yong, R. Kovacevic, Designing nozzle cross sections with off-line simulation for 3D abrasive waterjet machining, ASME, Proc. Fluids Eng. Div. 2 (1996) 503–508.
[9] R. Kovacevic, Z. Yong, Modeling of 3D abrasive waterjet machining, Jetting Technologies, published by Institution of Mechanical Engineers, (1996) 73–82.
[10] J.G.A. Bitter, A study of erosion phenomena: part I, Wear 6 (1963) 5–21.
[11] J.G.A. Bitter, A study of erosion phenomena: part II, Wear 6 (1963) 169–190.
[12] I. Finnie, A. Levy, D.H. McFadden, Fundamental Mechanisms of the erosive wear of ductile metals by solid particles, in: W.F. Alfer (ed.), ASTM STP664, ASTM, Philadelphia, PA, 1979, pp. 36–58.
[13] M. Hashish, A model for abrasive-waterjet (AWJ) machining, ASME J. Eng. Mater. Technol. 111 (1989) 154–162.
[14] Z. Yong, R. Kovacevic, Effects of water-mixture film on impact contact in abrasive waterjet machining, Int. J. Mech. Sci., in press (1996).
[15] H.M. Clark, L.C. Burmeister, The influence of the squeeze film on particle impact velocities in erosion, Int. J. Impact Eng. 3 (1992) 415–426.
[16] R.M. Bowen, Introduction to Continuum Mechanics for Engineers, Plenum, New York, 1989.
[17] S.P. Raju, M. Ramulu, A transient model for material removal in the abrasive waterjet machining process, Proc. of the 7th American Waterjet Conference, published by American Waterjet Society, St. Louis, USA, (1993) 141–155.
[18] I.H. Shames, Mechanics of Fluid, McGraw-Hill, New York, 1962.
[19] I.G. Currie, Fundamental Mechanics of Fluid, McGraw-Hill, New York, 1993.
[20] R. Kovacevic, Monitoring of depth of abrasive waterjet penetration, Int. J. Mach. Tools Manufac. 1 (1992) 55–72.